

- █ 右侧相邻主题与左侧同级主题，并列，但主题不同
- █ 右侧相邻主题与左侧同级主题，并列，且主题相同
- █ 右侧相邻主题与左侧同级主题，并列，且主题相同；或是左侧相邻主题的 sub 子主题

Nonlinear Diatomic Metasurface for Real and Fourier Space Image Encoding

Ningbin Mao, Junhong Deng, Xuecai Zhang, Yutao Tang, Mingke Jin, Yang Li, Xuan Liu, Kingfai Li, Tun Cao, Kokwai Cheah, Hong Wang, Jack Ng, and Guixin Li*



Cite This: <https://dx.doi.org/10.1021/acs.nanolett.0c02910>



Read Online

ACCESS |

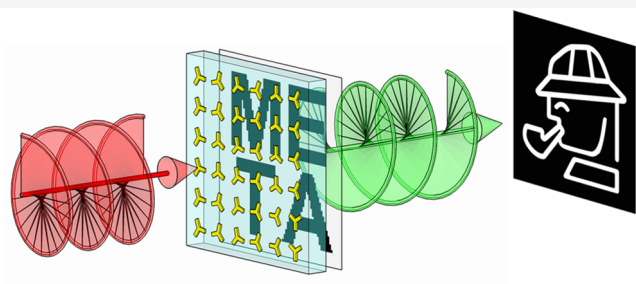
Metrics & More

Article Recommendations

Supporting Information

ABSTRACT: In linear optics, the metasurface represents an ideal platform for encoding optical information because of its unprecedented abilities of manipulating the intensity, polarization, and phase of light wave with subwavelength meta-atoms. However, controlling various degrees of freedom of light in nonlinear optics remains elusive. Here, we propose a nonlinear plasmonic metasurface working in the near-infrared regime that can simultaneously encode optical images in the real and Fourier spaces. This is achieved by designing a diatomic meta-molecule, which enables the independent control of the nonlinear geometric phase, polarization, and intensity of second harmonic waves. The proposed nonlinear diatomic metasurface provides an ultracompact platform for implementing multidimensional optical information encoding and may hold great potential in optical information security and optical anticounterfeiting.

KEYWORDS: optical metasurfaces, holography, nonlinear metasurfaces, plasmonics



Encoding optical information with an ultrathin device would enable a broad range of applications such as optical image encryption, optical communications, and so on. Among various strategies, metasurface technology already shows promising potentials in achieving multidimensional optical information encoding.¹ Photonic metasurfaces, which are made of subwavelength meta-atoms,² hold excellent capabilities in manipulating the intensity, phase, and polarization of light with subwavelength meta-atoms.³ In the linear optical regime, metasurfaces are widely used to encode optical information through optical holography.⁴ Although single-layer plasmonic metasurfaces have deep subwavelength thickness and are more compatible with the mature CMOS technology,⁵ they suffer from large optical losses. To avoid such limitations, researchers have extensively explored the metal-dielectric-metal (MIM) trilayer⁶ and single-layer all-dielectric metasurfaces⁷ to achieve high-efficiency beam deflection,^{8,9} meta-holography,¹⁰ and metalenses.¹¹ In the previous metasurface devices, their optical responses are mainly controlled through the manipulation of the phase properties, either by geometric Pancharatnam–Berry (P–B) phase,^{12–14} or by dynamic phase¹⁵ of light. By judiciously designing the meta-atoms, polarization multiplexed holographic images could be recorded in one metasurface device.^{16,17} In addition, through manipulating both the amplitude and phase information on light, simultaneous encryption of real and Fourier space images^{18–20} have been achieved on the dielectric metasurface platform.

On the other hand, the nonlinear frequency conversions by the metasurface may open new routes for advanced information encoding technologies.^{21–24} Compared with the established abilities to control the intensity, polarization, and phase of light in linear optics, the simultaneous control of these three degrees of freedom is challenging.^{25–27} Fortunately, this issue could be solved with the nonlinear geometric Pancharatnam–Berry phase.^{28,29} The spin-controlled nonlinear optical holography and nonlinear spin–orbit interactions have been successfully achieved by using both the plasmonic^{30,31} and the silicon-based dielectric metasurfaces.³² For the amplitude modulations, the interference effect of the nonlinear waves from the diatomic meta-molecule can be deployed. In this way, the geometric phase controlled nonlinear image encryption in the real space is accomplished.³³ Nevertheless, the nonlinear optical encoding in both real and Fourier spaces remains unexplored.

Here, we propose to simultaneously encode the real space and the holographic images by using a nonlinear diatomic metasurface. The meta-molecules are made from a pair of gold meta-atoms with C3 rotational symmetry. For a meta-atom

Received: July 14, 2020

Revised: September 8, 2020

Published: September 9, 2020

with certain rotational angle, the second harmonic generation (SHG) wave exhibits a spin-controlled geometric phase. The interference between the SHG waves in a meta-molecule will result in the amplitude modulations. As a result, we can simultaneously control the intensity and phase of the SHG wave by using a diatomic meta-molecule as a building block. On the basis of a self-developed holography code, we successfully encoded a real space and a holographic image by utilizing the plasmonic diatomic metasurface (Figure 1a). The nonlinear diatomic metasurface represents an important platform for multidimensional optical information encryptions, complex wavefront engineering, and so on.

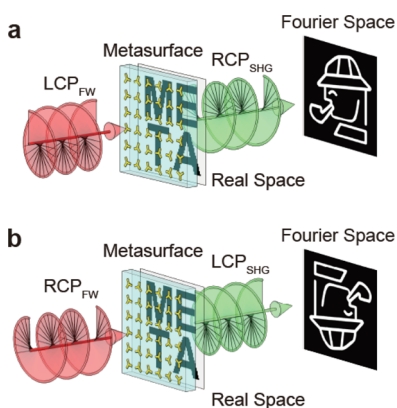


Figure 1. Nonlinear diatomic metasurface for real and Fourier space image encoding. Under the pumping of a circularly polarized fundamental wave (FW), the SHG wave with opposite handedness is generated on the nonlinear metasurface. By controlling the phase, polarization, and amplitude of the SHG wave, we are capable of encoding both the real space image of “META” and a holographic image of the portrait of Holmes in the Fourier space. By using the FW with LCP and RCP states, the two holographic images of “Holmes” show centrosymmetric characteristics.

RESULTS AND DISCUSSION

Geometric Phase-Controlled Nonlinear Metasurface Holography. First, we studied the geometric phase-controlled nonlinear metasurface holography by using the C3 gold nanostructure as a meta-atom. It is known that the spin state of the SHG wave from a C3 gold meta-atom has opposite handedness to that of the fundamental wave (FW).²³ On the basis of the principles of the geometric P–B phase in nonlinear optics, the phase term φ of the SHG wave are governed by the orientation angle θ of the C3 meta-atom. The relation between the nonlinear phase φ and the orientation angle θ satisfy $\varphi = 3\sigma\theta$ where $\sigma = +1$ and -1 represent the left circular polarization (LCP) and right circular polarization (RCP) states, respectively.²³ First, we demonstrate a phase-controlled computer-generated hologram (CGH) by using the concept of nonlinear geometric P–B phase (Figure 2). The “YinYang” pattern (Figure 2a) is chosen as the target image. In Figure 2b, the required phase profile for the metasurface hologram, with 16 phase levels ranging from $-\pi$ to π , is calculated using the standard Gerchberg–Saxton (GS) algorithm.³⁴ Then, based on the concept of spin-controlled nonlinear geometric phase, we are able to determine the position-dependent orientation angles of the C3 gold meta-atom. Figure 2c shows the scanning electron microscopy (SEM) image of the gold metasurface (see Methods).

The nonlinear optical properties of the diatomic metasurface hologram are then characterized by normally illuminating the plasmonic metasurface with a femtosecond laser (Figure S1). Before we do the SHG measurements. The optical transmittance of the “YinYang” metasurface is measured by using the Fourier Transform Infrared Spectrometer (FTIR). As shown in Figure S2b, the plasmonic resonances at shorter wavelengths are around 1126 nm (H–H) and 1100 nm (V–V), respectively. In comparison, the two resonant dips at longer wavelength are around 1376 nm (H–H) and 1382 nm (V–V), respectively. These characteristic modes are due to the

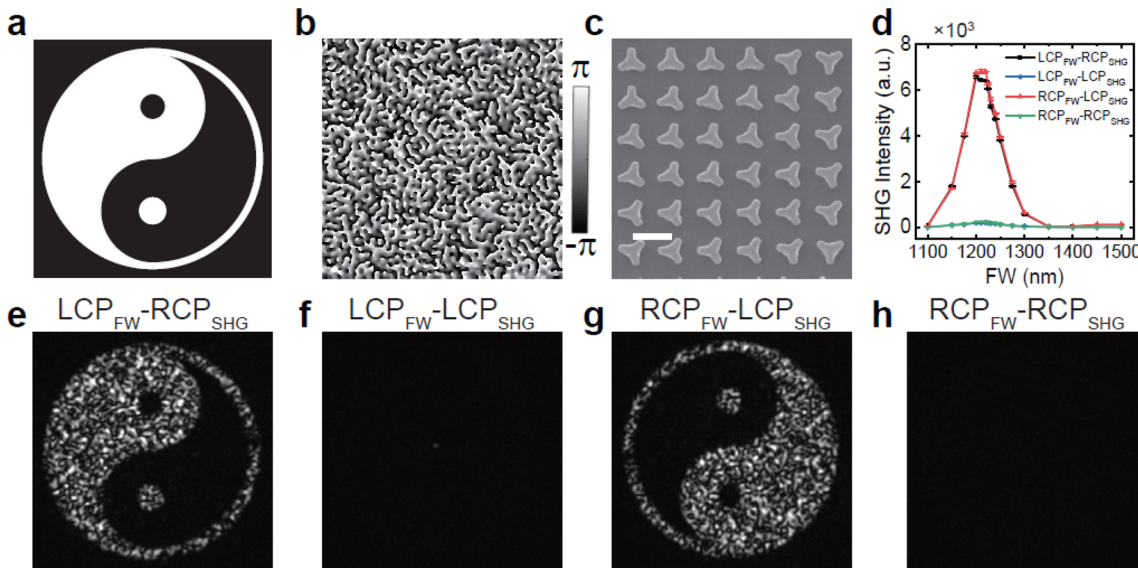


Figure 2. Geometric phase-controlled nonlinear metasurface holography. (a) Target image “YinYang” pattern. (b) Required phase distribution for generating the holographic image in (a). (c) SEM image of the metasurface. Scale bar: 500 nm. (d) Measured SHG responses of the metasurface shown in (c). The maximum SHG intensity is observed at the fundamental wavelength of 1210 nm. Different combination of circular polarization states of FW and SHG waves are recorded. (e–h) Measured SHG holographic images with different combinations of circular polarization states. The fundamental wavelength is 1210 nm.

plasmonic resonances at the gold–ITO interface (shorter wavelength) and gold–air interface (longer wavelength), respectively.³⁵ However, compared to the results in ref. 35, they are much shallower as the orientation directions of the C3 meta-atoms in a hologram device are very random. We measured the wavelength-dependent SHG intensities by scanning the fundamental wavelengths (FWs) from 1100 to 1500 nm. From the measured polarization resolved results in Figure 2d, we can see that the SHG waves with opposite handedness to that the FWs are much stronger compared to their counterparts, as required by the symmetry selection rules for harmonic generations.²³ The maximum intensity of the SHG wave appears at the wavelength of 1210 nm, which is ascribed to the epsilon-near-zero enhanced nonlinear optical process in the gold–ITO hybrid plasmonic metasurface.³⁵ The SHG holographic images are then recorded by a home-built setup, in which the FW at wavelength of 1210 nm is used as the illumination source. As shown in Figure 2e–h, the intensity of the SHG holographic images also follow the symmetry selection rules discussed previously. In Figure 2e, g, by flipping the spin states of FWs, the bright and dark regions of the two SHG holographic images are switched. This phenomenon is due to the nonlinear phase profiles being spin dependent. A similar effect on a geometric phase metasurface hologram was also observed before, but in the linear optical regime.⁴

Interference of SHG Waves from the Diatomic Metasurface. In previous section, we have demonstrated the nonlinear metasurface holography by using the single C3 meta-atom in a unit-cell. Here, we attempt to control both amplitude and phase of the SHG holographic images generated by the gold metasurfaces. This target can be realized by using a diatomic meta-molecule as the building block. As shown in Figure 3a, the diatomic nonlinear polarizability of the meta-molecule is described by the following equation

$$\alpha_{\text{SHG}}(-\sigma) \propto \exp(i3\sigma\theta_1) + \exp(i3\sigma\theta_2)$$

$$= 2\cos\frac{3\sigma(\theta_1 - \theta_2)}{2} \exp\left(i3\sigma\frac{\theta_1 + \theta_2}{2}\right)$$

represent the in-plane orientation angles of the two meta-atoms. The amplitude of SHG wave is proportional to $\cos(3\Delta/2)$ where $\Delta = \theta_1 - \theta_2$ is the orientation angle difference between the two meta-atoms. It is interesting that the weighted phase of the SHG wave $\Phi = 3\sigma\frac{\theta_1 + \theta_2}{2}$ which depends on the spin state of the FW and the sum of θ_1 and θ_2 can be observed. Thus, both the intensity and phase of the SHG waves can be controlled through adjusting θ_1 and θ_2 , respectively. We stress that although the nonlinear diatomic meta-molecule was also used for real space image encoding, a holographic image cannot be simultaneously encoded when the weighted nonlinear phase was neglected.³³

To verify the light-field-controlling capability of the meta-molecule, we design three nonlinear metasurface holograms, each with different predefined SHG intensities. The corresponding angle differences between θ_1 and θ_2 are 0, 30, and 60° for the three metasurfaces. For a target image CaTorch (a cat-like torch) shown in Figure 3b, the phase distribution for a holographic image projection is calculated by using the GS algorithm and shown in Figure 3c. For FW with LCP state, both the weighted phase and the relative phase of the SHG waves can be calculated, which are in turn used to obtain the orientation angles of the position-dependent diatomic meta-molecules. Figure 3d–f are SEM images of the metasurfaces: Cat-A, Cat-B, and Cat-C, respectively. To fabricate a

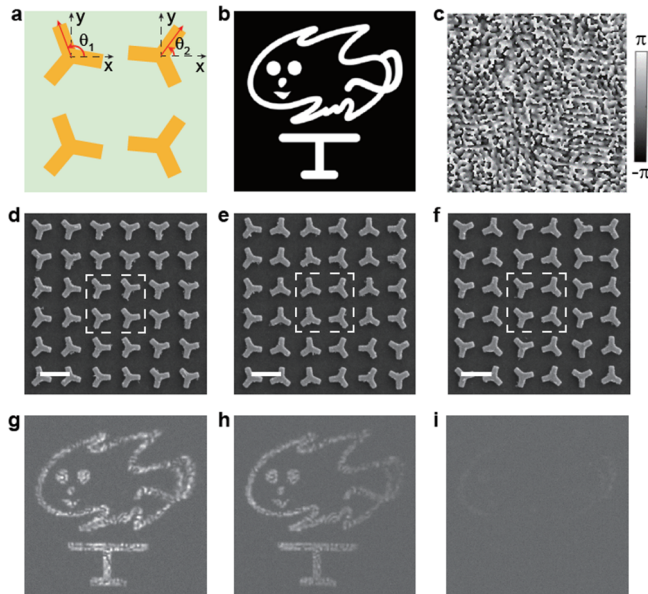


Figure 3. Interference effect of the SHG waves in the diatomic metasurface holography. (a) Unit cell of a diatomic nonlinear metasurface. The weighted and relative phase of the SHG waves are controlled by the orientation angles θ_1 and θ_2 of the two C3 gold meta-atoms. The orientation angles of the meta-atoms in all the metasurface holograms vary from 0° to 120° at a step of 15°. The size of each meta-molecule is set to be 1000 nm × 1000 nm. The length and width of each arm of a meta-atom are 180 and 80 nm, respectively. (b) Target image is a cat-like torch (CaTorch). (c) The required phase distribution of the SHG wave to reconstruct the holographic image CaTorch. (d–f) SEM images of three nonlinear metasurface holograms: Cat-A, Cat-B, and Cat-C, respectively (scale bar, 500 nm). Angle difference between two meta-atoms in a unit cell is 0, 30, and 60°, respectively. (g–i) Measured SHG holographic images with different SHG intensities. Under the excitation of LCP FW at wavelength of 1220 nm, the SHG wave has a RCP state.

metasurface device with a square shape, we repeated the diatomic meta-molecule once in vertical direction to form a 2 × 2 unit cell, which is illustrated by the dashed lines in Figure 3d–f, respectively. The measured intensities of right circularly polarized SHG holographic images in Figure 3g–i agree well with the theoretical predictions (Figures S5). At fundamental wavelength of ~1200 nm (Figure S4), the SHG conversion efficiency on the Cat-A metasurface is measured to be 1.39×10^{-9} for the pumping power of 4.77 mW.

Nonlinear Image Encoding in Real and Fourier Spaces. To further demonstrate the capabilities enabled by controlling the degrees of freedom of nonlinear waves using the diatomic metasurface, we explore the simultaneous encoding of both real space and Fourier space images. The design principle of CGH is based on the combination of the iteration algorithm³⁶ and the Fresnel–Kirchhoff diffraction formula (Figure S5).³⁷ As shown in Figure 4a, b, the word “META” and a portrait of Holmes are the target images for encoding in the real and Fourier spaces, respectively. Under normal incidence of the FW, the real space image of META at the second harmonic frequency can be differentiated from the bright background due to the destructive interference of SHG waves. In Figure 4c, the required phase distribution of the SHG wave for the Holmes portrait in the Fourier space is calculated by using a modified iteration algorithm for holographic image projection. Figure 4d shows the SEM

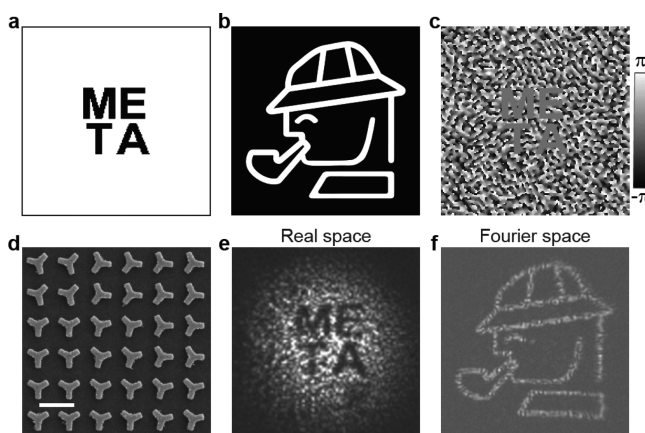


Figure 4. Nonlinear image encoding in real and Fourier spaces by using the diatomic metasurface. (a, b) Target image in real space and the holographic image in Fourier space. (c) Calculated phase profile of the diatomic metasurface hologram. (d) SEM image of the nonlinear metasurface device. Scale bar: 500 nm. (e, f) Measured real and Fourier space images at SH frequency. The FW at wavelength of 1220 nm is left circularly polarized, whereas the SHG signal has opposite handedness to that of FW.

image of the metasurface device. Under the illumination of the left circularly polarized FW at wavelength of 1220 nm, the right circularly polarized SHG wave at wavelength of 610 nm can be generated. Figure 4e shows the real space image “META” at the SHG frequency, which is experimentally observed on the metasurface plane. Meanwhile, a clear SHG holographic image of Holmes’s portrait is projected to the Fourier plane (Figure 4f). This indicates a good reconstruction of the image through nonlinear optical process as shown in Figure 4b. Both real and Fourier space images are recorded by using four polarization combinations (Figure S6).

CONCLUSION

To summarize, we propose a nonlinear diatomic metasurface platform, which is capable of achieving multidimensional optical information encoding. Both the relative phase and weighted phase of the SHG waves from a diatomic meta-molecule could be controlled by adjusting the rotational angles of the gold C3 meta-atoms. In this way, we acquire the ability to simultaneously manipulate the phase, polarization, and amplitude of nonlinear waves with a novel yet simple building block. By designing a nonlinear diatomic metasurface working at the second harmonic frequency, we demonstrate the polarization and amplitude-controlled nonlinear holography, and the nonlinear information encoding in both real and Fourier spaces. By judiciously choosing the appropriate symmetry and materials for the meta-atoms, the proposed methodology can be applied to other nonlinear optical processes. The ultrathin nonlinear diatomic metasurface serves as an interesting platform for on-chip manipulation of nonlinear waves and may hold great potential in optical information security, information processing, and so on.

METHODS

Design Principles of the Metasurface Holograms. If one of the long arms of the C3 meta-atom is along x -axis, the phase of the SHG wave generated on the meta-atom can be defined as zero. First, the phase distribution $\varphi(x, y)$ of the “YinYang” metasurface is obtained through computer-

generated hologram method, then the spatially variant C3 meta-atoms with orientation angle $\theta = \varphi/3\sigma$ are used to replace the required phase distribution. The fabrication data, which includes both the orientation information and the geometrical parameters, are then generated. Very similarly, once we have the design of the diatomic meta-molecule, the same procedures are used to design the metasurface devices in Figures 3 and 4.

Fabrication of Nonlinear Metasurfaces. The nonlinear diatomic metasurfaces are fabricated by using the electron-beam lithography technique. The electron resist with a film thicknesses of 120 nm is coated onto the ITO glass. The patterns of the metasurface are then written into the resist in the electron beam lithography process. The length and width of the nanorods of the C3 meta-atoms are around 180 and 80 nm. Each unit cell of the metasurface is a 500 nm \times 500 nm square cell. The patterned metasurface devices are successively immersed into the developer and fixative solution isopropyl alcohol (IPA), respectively. Then, a 30 nm thick Au film is deposited on the resist using the electron beam evaporation method. Finally, the electron beam resist is striped by the lift-off process with acetone.

Nonlinear Optical Measurements. An in-house developed optical measurement system is utilized to measure the nonlinear optical properties of the metasurfaces. The femtosecond laser has a repetition frequency of 80 MHz and a pulse duration ~ 250 fs. The circularly polarized FW is focused onto the metasurface with a spot diameter about 20 μm by a 4 \times objective lens. Then, the SHG waves pass through a 10 \times objective (Olympus, NA = 0.25) and analyzed by a quarter wave plate and a linear polarizer. A color filter (FESH800) is used to block the transmitted FW, the SHG waves are finally detected by the Andor spectrometer.

In the nonlinear imaging experiment, the 4 \times objective is replaced by a lens with a focal length $f = 250$ mm. The polarization resolved SHG images in both the real and Fourier spaces are recorded by a sCMOS camera. For the real space measurement, the metasurface is mounted at the focal point of a 10 \times objective. After passing through the objective, the SHG wave is finally focused by a tube lens with $f = 100$ mm. In this case, the camera is at the focal plane of the tube lens to capture the real space image. For the Fourier space measurement, the positions of both the metasurface and the collection objective lens are fixed. The image at the back focal plane of the objective can then be relayed by the tube lens. By finely moving the sCMOS camera to a distance that is longer than 100 mm, we are able to record the holographic image at the Fourier plane.

ASSOCIATED CONTENT

Supporting Information

The Supporting Information is available free of charge at <https://pubs.acs.org/doi/10.1021/acs.nanolett.0c02910>.

Nonlinear optical measurements; optical properties of the “YinYang” metasurface; interference effect of SHG waves and the nonlinear diatomic metasurface holography; SHG intensities of nonlinear diatomic metasurface holograms; modified iteration algorithm combined with diffraction formula; nonlinear image encoding in the real and Fourier spaces by using the diatomic metasurface (PDF)

AUTHOR INFORMATION

Corresponding Author

Guixin Li — Department of Materials Science and Engineering, Shenzhen Institute for Quantum Science and Engineering, Southern University of Science and Technology, Shenzhen 518055, China;  orcid.org/0000-0001-9689-8705; Email: ligx@sustech.edu.cn

Authors

Ningbin Mao — Department of Materials Science and Engineering, Southern University of Science and Technology, Shenzhen 518055, China; Department of Physics and Institute of Advanced Materials, Hong Kong Baptist University, Hong Kong, China

Junhong Deng — Department of Materials Science and Engineering, Shenzhen Institute for Quantum Science and Engineering, Southern University of Science and Technology, Shenzhen 518055, China

Xuecai Zhang — Department of Materials Science and Engineering, Southern University of Science and Technology, Shenzhen 518055, China

Yutao Tang — Department of Materials Science and Engineering, Southern University of Science and Technology, Shenzhen 518055, China; Department of Physics and Institute of Advanced Materials, Hong Kong Baptist University, Hong Kong, China

Mingke Jin — Department of Materials Science and Engineering, Southern University of Science and Technology, Shenzhen 518055, China

Yang Li — Department of Materials Science and Engineering, Southern University of Science and Technology, Shenzhen 518055, China; School of Optoelectronic Engineering and Instrumentation Science, Dalian University of Technology, Dalian 116024, China

Xuan Liu — Department of Materials Science and Engineering, Southern University of Science and Technology, Shenzhen 518055, China

Kingfai Li — Department of Materials Science and Engineering, Southern University of Science and Technology, Shenzhen 518055, China

Tun Cao — School of Optoelectronic Engineering and Instrumentation Science, Dalian University of Technology, Dalian 116024, China;  orcid.org/0000-0003-3536-0092

Kokwai Cheah — Department of Physics and Institute of Advanced Materials, Hong Kong Baptist University, Hong Kong, China

Hong Wang — Department of Materials Science and Engineering, Shenzhen Engineering Research Center for Novel Electronic Information Materials and Devices, Southern University of Science and Technology, Shenzhen 518055, China

Jack Ng — Department of Physics, Southern University of Science and Technology, Shenzhen 518055, China

Complete contact information is available at:

<https://pubs.acs.org/10.1021/acs.nanolett.0c02910>

Author Contributions

N.M., J.D., and X.Z. contributed equally. G.L. proposed the idea. N.M., X.Z., X.L., and Y.T. developed the code and methods for designing the metasurface hologram. J.D., N.M., and M.J. made the metasurface devices. K.L., Y.T., N.M., X.Z., Y.L., and G.L. measured the linear and nonlinear optical properties of the devices. N.M., X.L., Y.T., H.W., J.N., and G.L.

wrote the manuscript. All authors participated in the discussions and conducted the data analysis.

Notes

The authors declare no competing financial interest.

ACKNOWLEDGMENTS

G.L. is financially supported by National Natural Science Foundation of China (91950114, 11774145), Guangdong Provincial Innovation and Entrepreneurship Project (2017ZT07C071), Applied Science and Technology Project of Guangdong Science and Technology Department (2017B090918001). K. C. would like to thank Hong Kong Research Grants Council (GRF: 12303217). T. C. is supported by LiaoNing Revitalization Talents Program with grant number (XLYC1807237). H. W. and G. L. acknowledge the financial support from Shenzhen DRC project [2018]1433.

REFERENCES

- (1) Li, J.; Kamin, S.; Zheng, G.; Neubrech, F.; Zhang, S.; Liu, N. Addressable metasurfaces for dynamic holography and optical information encryption. *Sci. Adv.* **2018**, *4*, No. eaar6768.
- (2) Yu, N.; Genevet, P.; Kats, M. A.; Aieta, F.; Tetienne, J.-P.; Capasso, F.; Gaburro, Z. Light propagation with phase discontinuities: generalized laws of reflection and refraction. *Science* **2011**, *334*, 333–337.
- (3) Chen, H. T.; Taylor, A. J.; Yu, N. A review of metasurfaces: physics and applications. *Rep. Prog. Phys.* **2016**, *79*, 076401.
- (4) Deng, Z.-L.; Li, G. Metasurface optical holography. *Mater. Today Phys.* **2017**, *3*, 16–32.
- (5) Ni, X.; Kildishev, A. V.; Shalaev, V. M. Metasurface holograms for visible light. *Nat. Commun.* **2013**, *4*, 2807.
- (6) Zheng, G.; Mühlenernd, H.; Kenney, M.; Li, G.; Zentgraf, T.; Zhang, S. Metasurface holograms reaching 80% efficiency. *Nat. Nanotechnol.* **2015**, *10*, 308–312.
- (7) Staude, I.; Schilling, J. Metamaterial-inspired silicon nanophotonics. *Nat. Photonics* **2017**, *11*, 274–284.
- (8) Lalanne, P.; Astilean, S.; Chavel, P.; Cambril, E.; Launois, H. Blazed binary subwavelength gratings with efficiencies larger than those of conventional échelette gratings. *Opt. Lett.* **1998**, *23*, 1081–1083.
- (9) Lin, D.; Fan, P.; Hasman, E.; Brongersma, M. L. Dielectric gradient metasurface optical elements. *Science* **2014**, *345*, 298–302.
- (10) Arbabi, A.; Horie, Y.; Bagheri, M.; Faraon, A. Dielectric metasurfaces for complete control of phase and polarization with subwavelength spatial resolution and high transmission. *Nat. Nanotechnol.* **2015**, *10*, 937–943.
- (11) Khorasaninejad, M.; Chen, W. T.; Devlin, R. C.; Oh, J.; Zhu, A. Y.; Capasso, F. Metalenses at visible wavelengths: Diffraction-limited focusing and subwavelength resolution imaging. *Science* **2016**, *352*, 1190–1194.
- (12) Berry, M. V. The adiabatic phase and Pancharatnam's phase for polarized light. *J. Mod. Opt.* **1987**, *34*, 1401–1407.
- (13) Pancharatnam, S. Generalized theory of interference and its applications. *Proc. - Indian Acad. Sci., Sect. A* **1956**, *44*, 398–417.
- (14) Bomzon, Z.; Biener, G.; Kleiner, V.; Hasman, E. Space-variant Pancharatnam – Berry phase optical elements with computer-generated subwavelength gratings. *Opt. Lett.* **2002**, *27*, 1141–1143.
- (15) Chong, K. E.; Wang, L.; Staude, I.; James, A. R.; Dominguez, J.; Liu, S.; Subramania, G. S.; Decker, M.; Neshev, D. N.; Brener, I.; Kivshar, Y. S. Efficient polarization-insensitive complex wavefront control using Huygens' metasurfaces based on dielectric resonant meta-atoms. *ACS Photon.* **2016**, *3*, 514–519.
- (16) Wang, B.; Dong, F.; Yang, D.; Song, Z.; Xu, L.; Chu, W.; Gong, Q.; Li, Y. Polarization-controlled color-tunable holograms with dielectric metasurfaces. *Optica* **2017**, *4*, 1368–1371.
- (17) Deng, Z. L.; Deng, J.; Zhuang, X.; Wang, S.; Li, K.; Wang, Y.; Chi, Y.; Ye, X.; Xu, J.; Wang, G. P.; Zhao, R.; Wang, X.; Cao, Y.;

Cheng, X.; Li, G.; Li, X. Diatomic metasurface for vectorial holography. *Nano Lett.* **2018**, *18*, 2885–2892.

(18) Overvig, A. C.; Shrestha, S.; Malek, S. C.; Lu, M.; Stein, A.; Zheng, C.; Yu, N. Dielectric metasurfaces for complete and independent control of the optical amplitude and phase. *Light: Sci. Appl.* **2019**, *8*, 92.

(19) Bao, Y.; Yu, Y.; Xu, H.; Guo, C.; Li, J.; Sun, S.; Zhou, Z. K.; Qiu, C. W.; Wang, X. H. Full-colour nanoprint-hologram synchronous metasurface with arbitrary hue-saturation-brightness control. *Light: Sci. Appl.* **2019**, *8*, 95.

(20) Wei, Q.; Sain, B.; Wang, Y.; Reineke, B.; Li, X.; Huang, L.; Zentgraf, T. Simultaneous spectral and spatial modulation for color printing and holography using all-dielectric metasurfaces. *Nano Lett.* **2019**, *19*, 8964–8971.

(21) Kauranen, M.; Zayats, A. V. Nonlinear plasmonics. *Nat. Photon.* **2012**, *6*, 737–748.

(22) Lapine, M.; Shadrivov, I. V.; Kivshar, Y. S. Colloquium: nonlinear metamaterials. *Rev. Mod. Phys.* **2014**, *86*, 1093–1123.

(23) Li, G.; Zhang, S.; Zentgraf, T. Nonlinear photonic metasurfaces. *Nat. Rev. Mater.* **2017**, *2*, 17010.

(24) Koshelev, K.; Kruk, S.; Melik-Gaykazyan, E.; Choi, J. H.; Bogdanov, A.; Park, H. G.; Kivshar, Y. Subwavelength dielectric resonators for nonlinear nanophotonics. *Science* **2020**, *367*, 288–292.

(25) Keren-Zur, S.; Michaeli, L.; Suchowski, H.; Ellenbogen, T. Shaping light with nonlinear metasurfaces. *Adv. Opt. Photon.* **2018**, *10*, 309–353.

(26) Almeida, E.; Bitton, O.; Prior, Y. Nonlinear metamaterials for holography. *Nat. Commun.* **2016**, *7*, 12533.

(27) Gao, Y.; Fan, Y.; Wang, Y.; Yang, W.; Song, Q.; Xiao, S. Nonlinear Holographic all-dielectric metasurfaces. *Nano Lett.* **2018**, *18*, 8054–8061.

(28) Li, G.; Chen, S.; Pholchai, N.; Reineke, B.; Wong, P. W. H.; Pun, E. Y. B.; Cheah, K. W.; Zentgraf, T.; Zhang, S. Continuous control of the nonlinearity phase for harmonic generations. *Nat. Mater.* **2015**, *14*, 607–612.

(29) Segal, N.; Keren-Zur, S.; Hendler, N.; Ellenbogen, T. Controlling light with metamaterial-based nonlinear photonic crystals. *Nat. Photon.* **2015**, *9*, 180–184.

(30) Ye, W.; Zeuner, F.; Li, X.; Reineke, B.; He, S.; Qiu, C.-W.; Liu, J.; Wang, Y.; Zhang, S.; Zentgraf, T. Spin and wavelength multiplexed nonlinear metasurface holography. *Nat. Commun.* **2016**, *7*, 11930.

(31) Li, G.; Wu, L.; Li, K. F.; Chen, S.; Schlickriede, C.; Xu, Z.; Huang, S.; Li, W.; Liu, Y.; Pun, E. Y. B.; Zentgraf, T.; Cheah, K. W.; Luo, Y.; Zhang, S. Nonlinear Metasurface for simultaneous control of spin and orbital angular momentum in second harmonic generation. *Nano Lett.* **2017**, *17*, 7974–7979.

(32) Reineke, B.; Sain, B.; Zhao, R.; Carletti, L.; Liu, B.; Huang, L.; De Angelis, C.; Zentgraf, T. Silicon Metasurfaces for third harmonic geometric phase manipulation and multiplexed holography. *Nano Lett.* **2019**, *19*, 6585–6591.

(33) Walter, F.; Li, G.; Meier, C.; Zhang, S.; Zentgraf, T. Ultrathin nonlinear metasurface for optical image encoding. *Nano Lett.* **2017**, *17*, 3171–3175.

(34) Gerchberg, R. W.; Saxton, W. O. Practical algorithm for the determination of phase from image and diffraction plane pictures. *Optik* **1972**, *35*, 237–246.

(35) Deng, J.; Tang, Y.; Chen, S.; Li, K.; Zayats, A. V.; Li, G. Giant enhancement of second-order nonlinearity of epsilon-near-zero medium by a plasmonic metasurface. *Nano Lett.* **2020**, *20*, 5421–5427.

(36) Feldman, M. R.; Guest, C. C. Iterative encoding of high-efficiency holograms for generation of spot arrays. *Opt. Lett.* **1989**, *14*, 479–481.

(37) Goodman, J. W. *Introduction to Fourier Optics*; McGraw-Hill, 1995.